Multiscale Geopotential Solutions from CHAMP Orbits and Accelerometry

Martin J. Fengler[1], Willi Freeden[1], and Jürgen Kusche[2]

[1] TU Kaiserslautern, Geomathematics Group, 67653 Kaiserslautern, P.O. Box 3049, Germany
[2] TU Delft/DEOS, 2600 GB Delft, P.O. Box 5058, The Netherlands

Summary. CHAMP orbits and accelerometer data are used to recover the long- to medium-wavelength features of the Earth's gravitational potential. In this study we are concerned with analyzing preprocessed data in a framework of multiscale recovery of the Earth's gravitational potential, allowing both global and regional solutions. The energy conservation approach has been used to convert orbits and accelerometer data into in-situ potential. Our modelling is spacewise, based on (1) non-bandlimited least square adjustment splines to take into account the true (non-spherical) shape of the trajectory (2) harmonic regularization wavelets for solving the underlying inverse problem of downward continuation. Furthermore we can show that by adapting regularization parameters to specific regions local solutions can improve considerably on global ones. We apply this concept to kinematic CHAMP orbits, and, for test purposes, to dynamic orbits. Finally we compare our recovered model to the EGM96 model, and the GFZ models EIGEN-2 and EIGEN-GRACE01s.

Key words: CHAMP, Kinematic Orbit, PSO Orbit, Regional Gravitational Field Recovery, Tikhonov-Wavelet Regularization

1 Introduction

In this paper high-low satellite-to-satellite tracking (hi-lo SST) of a low Earth orbiter (LEO) for gravity recovery purposes is discussed from an alternative point of view, as originally proposed by W. Freeden [4]. More specifically, we are concerned with the determination of the Earth's external gravitational field from a given set of potential values along the orbit of CHAMP. We have obtained these potential values by applying an energy conservation approach, basically following [8], to GFZ PSO as well as to TUM kinematic CHAMP orbits. In order to translate the hi-lo SST problem into a rigorous mathematical formulation we will make use of the geometrical situation outlined in Fig. 1.

We have the following problem (see [4]): *Let there be known the potential values* $V(x), x \in \Gamma$*, for a subset* $\Gamma \subset \Sigma^{ext}$ *of points at the orbit positions of the LEO. Find an approximation* U *to the geopotential field* V *on* $\overline{\Sigma^{ext}}$*, i.e. on and outside the Earth's surface, such that the difference of* V *and* U *is arbitrarily small on* $\overline{\Sigma^{ext}}$ *in terms of the underlying function spaces. In addition we require* $V(x) = U(x)$ *for all* $x \in \Gamma$. Existence, uniqueness, and well-posedness of the problem are discussed in [4] and the references therein.

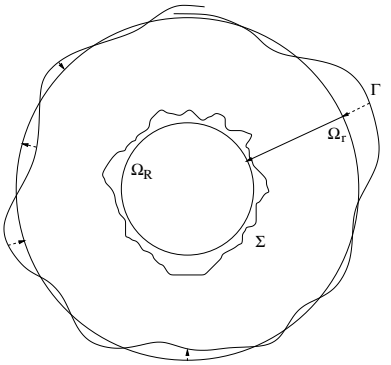

Fig. 1. Illustration of the geometrical configuration.

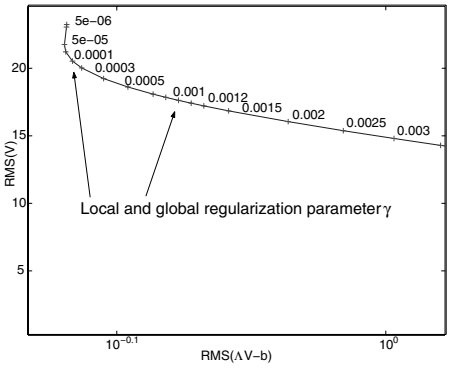

Fig. 2. Local L-curve for the region shown in Fig. 3, in $\mathrm{Harm}_{25,\ldots,90}(\Omega_R)$.

In practice we are interested in computing global, and if possible, regionally improved gravity models from real CHAMP-data. In particular for the regional case our wavelet approach demonstrates advantages since it allows for the local choice of a regularization parameter. Thus, we apply locally adaptive regularization by virtue of multiresolution analysis using adequately constructed wavelets.

The three-dimensional coordinate system that we use throughout this study is the particular realization of the international terrestrial reference frame in which the CHAMP ephemeris are given. Let r be CHAMP's mean orbital altitude. The sphere in $\mathbb{R}^3$ with radius r around the origin is denoted by Ω_r, i.e. $\Omega_r = \{x \in \mathbb{R}^3 || x| = r\}$. For later use we reserve the name Ω_R to denote the Bjerhammar sphere (see Fig. 1). With Ω_r^{ext} we denote the exterior of Ω_r, while Ω_r^{int} is the interior of Ω_r. Further, in our modelling we will make use of two different spherical grids: The equiangular Driscoll-Healy grid [1] for numerical integration purposes, and the so–called Reuter grid [11] known from low discrepancy methods. The Reuter grid is important in our data selection strategy since it exhibits an almost equidistribution of the points on the sphere.

For extrapolation of the data $\{y_i, F_i\}, i = 1, \ldots, M$, i.e. M potential values along the orbit Γ to an integration grid on the sphere Ω_r we use a least square adjustment spline S, see for more details [2, 3, 10]. For this purpose we employ a Reuter grid $\{x_j\}, j = 1, \ldots, N \subset \Omega_R$ for locating the Abel-Poisson kernel K which is defined by

$$K_{\mathcal{H}(A,\Omega_R)}(x,y) = \frac{1}{4\pi R^2} \frac{1-h^2}{(1+h^2-2h(x\cdot y))^{3/2}} \,. \tag{1}$$

The N coefficients of the spline $S = \sum_{j=1}^{N} a_j K(x_j, \cdot)$ follow from solving the overdetermined linear system

$$\sum_{j=1}^{N} a_j^N K_{\mathcal{H}}(x_i, y_j) = F_i, \quad i = 1, \ldots, M.$$

Sobolev Spaces: We will work in Sobolev spaces, as introduced in [5, 4], and assume in particular that the measured potential can be characterized as an element of the space $\mathcal{H}(A, \Omega_R)$ with symbol $A^\wedge(n) = h^{-n/2}$, $n \in \mathbb{N}_0$, $0 < h < 1$. This again leads immediately to the Abel-Poisson kernel, representing the reproducing kernel in $\mathcal{H}(h^{-n/2}, \Omega_R)$. It should be remarked that this kernel can be directly identified with the *upward continuation* operator. This operator facilitates mapping between $\mathcal{H}(A, \overline{\Omega_R^{ext}})$ and $\mathcal{H}(\Lambda^{-1}A, \overline{\Omega_r^{ext}})$, and can be interpreted as a pseudodifferential operator (PDO) defined on $\mathcal{H}(A, \overline{\Omega_R^{ext}})$ with the symbol $\Lambda^\wedge(n) = \left(\frac{R}{r}\right)^{n+1}$.

Tikhonov Regularization Scaling Functions: Now we consider the solution of the inverse problem given by $\Lambda V = G$, $V \in \mathrm{L}^2(\Omega_R)$, and $G \in \mathrm{L}^2(\Omega_r)$. As is well-known, cf. [4], this equation possesses an exponentially ill-posed pseudodifferential equation with an unbounded inverse operator Λ^{-1}. The idea of regularization is to replace the inverse operator by a more 'friendly' operator which yields an approximate solution. By operating directly on the singular values of Λ^{-1}, wavelets appear as a very appropriate tool to solve this problem. We obtain the J-level regularization of the potential V on Ω_R by evaluating the convolution $V_J = \Phi_J * G = \int_{\Omega_r} \Phi_J(\cdot, \eta) G(\eta) d\omega_r(\eta)$, where Φ_J denotes the J-level regularization and reconstruction Tikhonov scaling function:

Definition 1 (Tikhonov Scaling Function). *Let $P_n, n \in \mathbb{N}_0$ denote the Legendre polynomials as given by [5], and $\gamma_j, j \in \mathbb{N}_0$ a positive decreasing sequence with $\lim_{j\to\infty} \gamma_j = 0$. The Tikhonov regularization scaling function is defined by*

$$\Phi_j(x, y) = \sum_{n=0}^{\infty} \phi_j(n) \frac{2n+1}{4\pi Rr} \left(\frac{Rr}{|x||y|}\right)^{n+1} P_n\left(\frac{x}{|x|} \cdot \frac{y}{|y|}\right),$$

with $x \in \Omega_R, y \in \Omega_r$, and the symbol $\phi_j(n)$ is given by

$$\phi_j(n) = \frac{\Lambda^\wedge(n)}{(\Lambda^\wedge(n))^2 + \gamma_j}, \quad n = 0, 1, \ldots;\ j \in \mathbb{N}_0.$$

Since $\phi_j(n)$ decreases for increasing n, we may regard these functions just as low-pass filters - which is similar to Tikhonov regularization for ill-conditioned linear systems. The Tikhonov regularization wavelets are analogously obtained as bandpass filters, i.e. by the difference of two subsequent low-pass filters (see [4]).

2 Multiscale Geopotential Modelling from CHAMP Data

In the present study we consider two different CHAMP orbit data sets, covering several months in the year 2002. We work with dynamic PSO orbits provided kindly by

GFZ Potsdam, and with kinematic orbits computed by Drazen Svehla (IAPG, TU Munich) following the zero-differencing strategy. Whereas dynamic orbits basically represent a best-fit of GPS observations within an a–priori gravity field and provide a kind of test for our method, kinematic orbits are free of a-priori gravity information and the recovered gravity model should be free of any biases. These orbits have been converted to in-situ potential values following the energy conservation approach (cf. [8]), corrected for nonconservative forces using GFZ's accelerometer data products, and for astronomical and solid Earth tides according to IERS conventions, and ocean tides using GOT 99.2. That the energy balance approach can be successfully applied to gravity recovery from CHAMP has been proven meanwhile by several groups, cf. [7], [6], or [9]. By subtracting a reference potential up to degree 24 (from EGM96) we obtain residual potential values along the orbit. Finally, by using cubic approximating splines we try to suppress trends in the data which we believe are induced by remaining accelerometer drift effects.

Data Gridding with Splines: First, using the Abel-Poisson kernel with $h = 0.95$, we fit a least square adjustment spline to the residual potential along the satellite orbit. All data has been weighted equally, after applying a selection procedure. It is then possible to extrapolate these values to a Driscoll-Healy integration grid defined on the mean altitude sphere Ω_r (see Fig. 1). This essential step preserves the harmonicity in the data.

Solving the Inverse Problem and Reconstruction: From the previous step, we have now a set of gridded, *predicted measurements* on Ω_r. This allows us to compute a j-level regularization of the potential on Ω_R. However, we need an appropriate criterion for stopping the regularization, i.e. we have to balance the regularization error decreasing with higher scales, and the the reconstruction/prediction error increasing with higher scales. For this purpose we use the L-curve method, which in turn requires that we predict residual potential values in the spherical integration grid on Ω_r, by use of the recovered potential. Since $\|\cdot\|_{\mathcal{H}(A,\Omega_R)}$ is defined in the spectral domain, we prefer for regional applications the $\mathrm{L}^2(\Omega_R)-$norm which can easily be evaluated in the space domain. We plot the norm of the reconstructed potential (within $\mathrm{Harm}_{25,\ldots,90}(\Omega_R)$, see below) on the y-axis against the prediction residual from this potential to the orbit data on the x-axis (cf. Fig. 2). Locally, we calculate the RMS of the reconstructed potential values respectively the data residuals on a grid, which approximates the L^2-norm. It should be remarked that the time-consuming numerical integration in the wavelet transform is intrinsically data parallel. We exploit this by using an efficient parallel implementation. For an easier comparison of our solution with spherical harmonic models, we project the solution globally on $\mathrm{Harm}_{25,\ldots,50}(\Omega_R)$ and locally on $\mathrm{Harm}_{25,\ldots,90}(\Omega_R)$; that is we extract those spectral bands from our solution which can then directly compared to spherical harmonic expansions. The difference in the globally recovered potential compared to several models is given in Tab. 1 and 2.

Local Reconstruction Process: The Tikhonov scaling functions are strongly localizing on Ω_R. It is clear that only a small cap contributes in the reconstructing convolution, which resembles numerically a *local compact support*. It is the rea-

Table 1. Global potential differences from CHAMP-PSO data in $\mathrm{Harm}_{25,\ldots,50}$

$[\mathrm{m}^2/\mathrm{s}^2]$	EGM96	EIGEN-1s	EIGEN-2	EIGEN-GRACE01s
Median Abs. Diff.	2.918	2.900	2.407	2.467
Mean Abs. Diff.	3.825	3.727	3.283	3.274

Table 2. Global potential differences from CHAMPTUM kinematic data in $\mathrm{Harm}_{25,\ldots,50}$

$[\mathrm{m}^2/\mathrm{s}^2]$	EGM96	EIGEN-1s	EIGEN-2	EIGEN-GRACE01s
Median Abs. Diff.	2.888	3.257	2.620	2.552
Mean Abs. Diff.	3.785	4.027	3.416	3.258

son why we are able to compute a reconstruction of the gravitational potential in a desired area only. For a detailed description for the choices of the windows see [2].

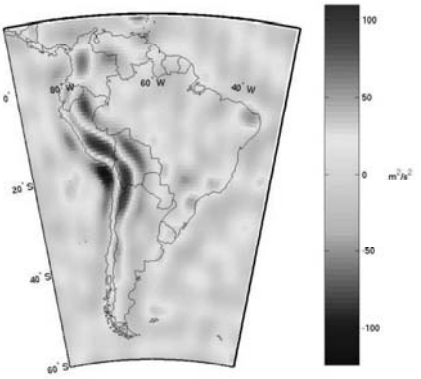

Fig. 3. Locally improved potential in $\mathrm{Harm}_{25,\ldots,90}(\Omega_R)$.

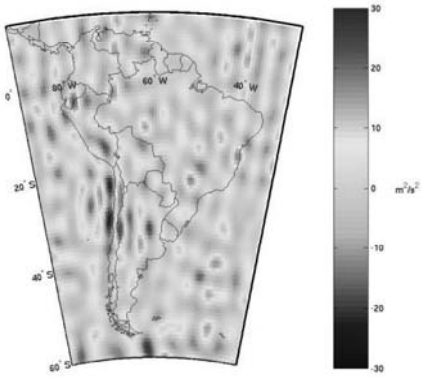

Fig. 4. Difference Fig. 3 and EIGEN-2 in $\mathrm{Harm}_{25,\ldots,90}(\Omega_R)$.

Local CHAMP Data Analysis: Global reconstructions show that differences to EIGEN-2 are located mainly in the high frequency parts, owing probably to regularization effects. Thus, we analyze a region of strong signal (see Fig. 3) and try to improve our global results locally. The locally obtained L-curve, Fig. 2, reveals that the regularization parameter obtained from a global L-curve is too large for this specific region, and high-frequent phenomena are over-smoothed. For more detail see [2]. Beyond this, the local L-curve indicates that $\gamma = 0.0001$ is an appropriate choice for this region. It turns out, that we are in fact able to improve our model locally. The maximum differences to EIGEN-1s and EIGEN-2 could be significantly decreased from ca. $60\frac{\mathrm{m}^2}{\mathrm{s}^2}$ to ca. $20\frac{\mathrm{m}^2}{\mathrm{s}^2}$ or even less, see Fig. 4. Remaining differences

can be assigned to regions of high signal variability in the Andes. It will be subject of future work to investigate 'trackiness' in the solutions.

3 Conclusion

We believe our results show that a spline-based wavelet method can be applied successfully to real CHAMP data. Beyond this, it should be outlined that our method can improve satellite-only models regionally by adapting the regularization procedure to the regional variability of the Earth's gravity field.

Acknowledgement. We are grateful to GFZ Potsdam for providing access to CHAMP data products. Thanks go also to IAPG, TU Munich, for providing kinematic orbits. Further we are indebted to Research Center Jülich and to ITWM-Fraunhofer Institute Kaiserslautern, for granting access to high–performance computing facilities.

References

1. Driscoll JR, Healy DM (1994) Computing Fourier Transforms and Convolutions on the 2-Sphere. Adv Appl Math *15*: 202–250.
2. MJ Fengler, Freeden W, Michel V (2003) The Kaiserslautern Multiscale Geopotential Model SWITCH-03 from Orbit Perturbations of the Satellite CHAMP and Its Comparison to the Models EGM96, UCPH2002_02_0.5, EIGEN-1s, and EIGEN-2. Geophys J Inter (accepted).
3. Freeden W (1981) On Approximation by Harmonic Splines. Manuscr Geod *6*: 193–244.
4. Freeden W (1999) Multiscale Modelling of Spaceborne Geodata. BG Teubner, Stuttgart, Leipzig.
5. Freeden W, Gervens T, Schreiner M (1998) Constructive Approximation on the Sphere (With Applications to Geomathematics). Oxford Science Publications, Clarendon, Oxford.
6. Gerlach C, Sneeuw N, Visser P, Svehla D (2003) CHAMP gravity field recovery with the energy balance approach: first results. in: Reigber C, Lühr H, Schwintzer P (eds), First CHAMP Mission Results for Gravity, Magnetic and Atmospheric Studies, Springer, Berlin: 134–139.
7. Han S-C, Jekeli C, Shum CK (2002) Efficient Gravity Field Recovery using in situ Disturbing Potential Observables from CHAMP. Geophys Res Lett *29(16)*: doi10.1029/2002GL015180.
8. Jekeli C (1999) The determination of gravitational potential differences from satellite-to-satellite tracking. Cel Mech Dyn Astron *75*: 85–101.
9. Kusche J, van Loon J (2004) Statistical assessment of Champ data and models using the energy balance approach. This volume.
10. Kusche J (2002) Inverse Probleme bei der Gravitationsfeldbestimmung mittels SST- und SGG-Satellitenmissionen. DGK Series C, No. 548, Munich.
11. Reuter R (1982) Über Integralformeln der Einheitssphäre und harmonische Splinefunktionen. Veröff Geod Inst RWTH Aachen, No. 33.